

larger or smaller than the two threshold values during the iterative decoding process, the calculations of the LLR, FR and BR are simpler than those of the MAP algorithm. Thus, the complexity and decoding time of iterative decoders are reduced, and the performance of the MMAP algorithm is almost the same as that of the MAP algorithm.

Acknowledgments: This work was supported by the Dongguk University research fund.

© IEE 2001

20 March 2001

Electronics Letters Online No: 20010486
DOI: 10.1049/el:20010486

Jun Lee and Jaemin Lee (*Department of Electronic Engineering, Dongguk University, 26 Pil-dong 3-ga, Chung-gu, Seoul, 100-715, Korea*)

E-mail: zlee@dgu.ac.kr

References

- BERROU, C., GLAVIEUX, A., and THITIMAJISHIMA, P.: 'Near Shannon limit error-correcting coding and decoding: turbo codes'. Proc. ICC, June 1993
- ROBERTSON, P., VILLEBRUN, E., and HOEHER, P.: 'A comparison of optimal and sub-optimal MAP decoding algorithms operating in the log domain'. Proc. ICC, June 1995

1.52 Tbit/s OCDM/WDM (4 OCDM × 19 WDM × 20 Gbit/s) transmission experiment

H. Sotobayashi, W. Chujo and K. Kitayama

1.52 Tbit/s OCDM/WDM (4 OCDM × 19 WDM × 20 Gbit/s) transmission based on simultaneous multi-wavelength optical encoding of a single supercontinuum source is experimentally demonstrated with 0.4 bit/s/Hz spectrum efficiency.

Introduction: Optical code division multiplexing (OCDM) provides a unique combination of attributes such as asynchronous transmission, secure communication, tell-and-go access protocol, soft capacity on demand, and a high degree of scalability [1, 2]. OCDM applications range from point-to-point transmission [3], multiple access [4], optical path network [5, 6], and label switching routing [7]. Key technologies for developing multi-Tbit/s OCDM systems are ultrafast optical encoding/decoding, ultrafast optical time-gating for interference noise suppression, and ultra-broadband source generation.

In this Letter we report 1.52 Tbit/s OCDM/WDM (4 OCDM × 19 WDM × 20 Gbit/s) transmission over an 80 km dispersion-compensated link based on simultaneous multi-wavelength optical encoding of a single supercontinuum (SC) source by exploiting a periodic impulse response from an optical encoder in the frequency domain. To the authors' knowledge, this is the highest transmission capacity obtained from OCDM/WDM transmission experiments.

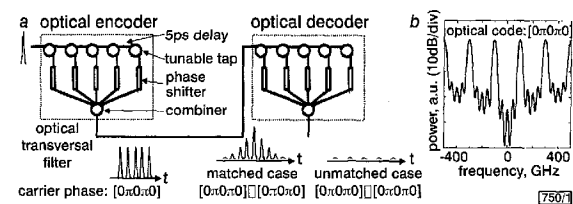


Fig. 1 Principle of OCDM based on time spread/despread using optical transversal filters and 200 GHz periodicity in impulse response of optical encoding in frequency domain

- OCDM using optical transversal filters
- 200 GHz periodicity

Operation principle: As shown in Fig. 1a, optical transversal filters are used as optical encoders and decoders. The transversal filter

consists of tunable taps, 5 ps delay lines, programmable binary optical phase shifters, and a combiner, all of which are monolithically integrated as a planar lightwave circuit. An optical code comprising a five-chip pulse BPSK pulse code sequence with a chip interval of 5 ps is generated [1]. The impulse response of the optical encoding has a periodicity of 200 GHz, because the chip interval of the optical encoder is 5 ps, as shown in Fig. 1b [8]. As a result, simultaneous multi-wavelength encoding having a WDM channel spacing of 200 GHz can be achieved using a single optical encoder when a broadband optical pulse such as an SC pulse is used as a chip pulse.

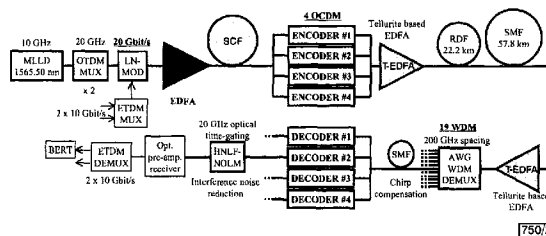


Fig. 2 Experimental setup

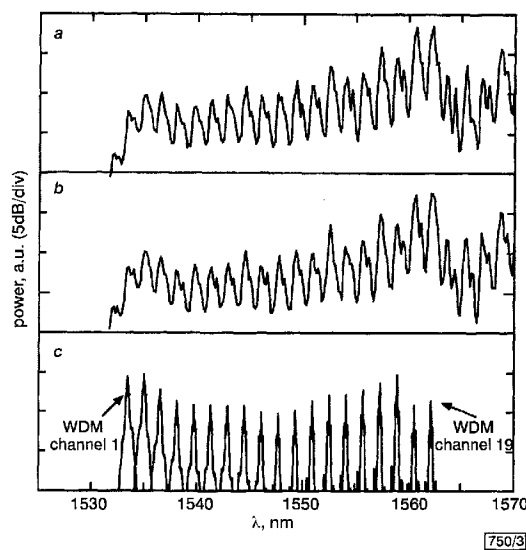


Fig. 3 Optical spectra before transmission, after transmission, and after WDM DEMUX and optical decoding

- Before transmission
- After transmission
- After WDM DEMUX and decoding

Experiments and results: Fig. 2 shows the experimental setup of our 1.52 Tbit/s OCDM/WDM (4 OCDM × 19 WDM × 20 Gbit/s) transmission experiment. A 10 GHz, 1.5 ps pulse train from a modelocked laser diode (MLLD) operating at 1565.50 nm was optically multiplexed to 20 GHz and modulated with a 20 Gbit/s $2^{23}-1$ PRBS. After being amplified to an average power of 1 W, the pulse train was launched into an SC fibre (SCF) [9]. The generated 20 Gbit/s SC signal was split into four, with each serving as the light source for simultaneous multi-wavelength optical encoding using the optical encoder. Four different optical encoded signals having a WDM channel spacing of 200 GHz, which corresponds to 0.4 bit/s/Hz spectrum efficiency. A Tellurite-based EDFA (T-EDFA) with three-stage amplification was used for broadband signal amplification and spectrum equalisation by adjusting the three-stage pump powers. The transmission line comprised a reversed-dispersion fibre (RDF) and singlemode dispersion fibre (SMF) pair. The total length was 80 km, the average zero dispersion wavelength was 1546.59 nm and the dispersion slope was 0.0087 ps/nm/km. After being amplified by a T-EDFA, it was wavelength demultiplexed (DEMUX) by a 19 channel arrayed wavelength grating (AWG) having a channel spacing of

200 GHz (channel 1: 1533.47 nm – channel 19: 1562.23 nm). After WDM DEMUX, frequency chirping was compensated for to compress the chip pulse using a 13.5 m SMF because the SC pulse was up-chirped [9]. It was then decoded by an optical decoder and optical time-gated using a 100 m highly nonlinear dispersion-shifted fibre (HNLF) based nonlinear optical loop mirror (NOLM) to suppress the interference noise as well as additive noise [1–3]. By using an HNLF, which has a high nonlinear coefficient and a low dispersion slope [10], we were able to minimise the walk-off problem between the control pulse and signal pulse. The control pulse used for 20 GHz optical time-gating was optically multiplexed in the time domain to 20 GHz using 10 GHz, 1.5 ps pulse trains from the MLLD at 1550.00 nm for gating of WDM channels 1–9, or 1540.00 nm for gating of WDM channels 10–19. The optical gating window ranged from 1.5 to 1.8 ps for all WDM channels.

Fig. 3 shows the optical spectra of the signals before transmission (upper trace), after transmission (middle trace), and after WDM DEMUX and optical decoding (lower trace). The -15 dB bandwidth of the SC spectrum was ~ 130 nm. The power difference in all WDM channels was ~ 6 dB after WDM DEMUX. Figs. 4a and b, respectively, show the streak camera trace and eye diagram of the decoded code $[0\pi 0\pi 0]$ of channel 10 (1547.72 nm) after 80 km transmission. The sharp peak of the matched code can be clearly seen in the centre, although interference noise severely distorted the signal-to-noise ratio. The sidelobes of the decoded signal were disturbed by the existence of cross-correlations of the other three unmatched codes, as can be seen in comparison with the only matched signal decoding (dotted line in Fig. 4a). Figs. 4c and d show the optical time-gated decoded signals. By optical time-gating the mainlobe of the matched correlation waveforms, the interference noise was greatly reduced and the signal-to-noise ratio greatly improved. Fig. 4e shows the measured BERs of the decoded 4 OCDFM \times 19 WDM ($=76$) data signals. For all measured signals, the BERs were less than 1×10^{-9} .

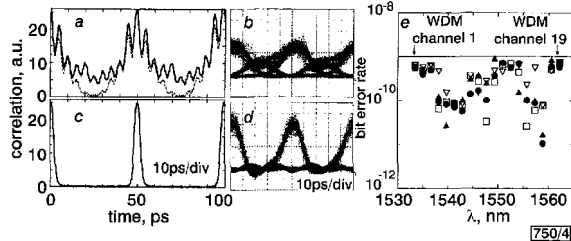


Fig. 4 Streak camera traces and eye diagrams of decoded signal from channel 10, optical time-gated decoded signal and measured BER of decoded 4 OCDFM \times 19 WDM ($=76$) data signals

a Decoded signal from channel 10

— 4 OCDFM

..... 1 OCDFM

b Streak camera trace (upper) and eye diagram (lower) of signal from channel 10

c Optical time-gated coded signal

d Streak camera trace (upper) and eye diagram (lower) of coded signal

e Measured BER of decoded 4 OCDFM \times 19 WDM data signals

● 00000

□ 00 π 0

▲ 0 π 0 π 0

▽ 0 π 0 π

Conclusion: 1.52 Tbit/s OCDFM/WDM (4 OCDFM \times 19 WDM \times 20 Gbit/s) signals each having five-chip pulses with WDM channel spacing of 200 GHz have been generated by simultaneous multi-wavelength optical encoding of a single SC source by exploiting the periodic impulse response of an optical encoder in the frequency domain. Error-free transmission was achieved by introducing a novel interference noise suppression technique based on ultrahigh-speed optical time-gating. Using only the C-band wavelength region, we succeeded in obtaining 1.52 Tbit/s (4 OCDFM \times 19 WDM \times 20 Gbit/s) OCDFM/WDM transmission over 80 km with 0.4 bit/s/Hz spectrum efficiency. By increasing the number of optical codes and WDM channels, utilising the S- and L-band wavelength regions, and employing polarisation multiplexing, OCDFM/WDM transmission at > 12 Tbit/s would be feasible.

© IEE 2001

Electronics Letters Online No: 20010483

DOI: 10.1049/el:20010483

H. Sotobayashi and W. Chujo (Communications Research Laboratory, Independent Administrative Institution, 4-2-1, Nukui-Kita, Koganei, Tokyo 184-8795, Japan)

E-mail: soba@crl.go.jp

K. Kitayama (Osaka University, Department of Electronics and Information Systems, 2-1, Yamadaoka, Suita, Osaka 565-0871, Japan)

References

- 1 KITAYAMA, K., SOTOBAYASHI, H., and WADA, N.: 'Optical code division multiplexing (OCDFM) and its application to photonic networks', *IEICE Trans. Fundam.*, 1999, **E82-A**, (12), pp. 2616–2626
- 2 SAMPSON, D.D., PENDOCK, G.J., and GRIFFIN, R.A.: 'Photonic code-division multiple-access communications', *Fiber Integrat. Opt.*, 1997, **16**, pp. 129–157
- 3 SOTOBAYASHI, H., CHUJO, W., and KITAYAMA, K.: '3 \times 10 Gbit/s OCDFM transmission at 1550 nm band over 150 km standard fiber using midspan optical phase conjugation'. OECC'2000, 2000, Paper 14A2-4.
- 4 SOTOBAYASHI, H., and KITAYAMA, K.: 'Broadcast-and-select OCDFM/WDM network by using 10 Gbit/s spectrum-sliced supercontinuum BPSK pulse code sequences', *Electron. Lett.*, 1999, **35**, (22), pp. 1966–1967
- 5 KITAYAMA, K.: 'Code division multiplexing lightwave networks based upon optical code conversion', *IEEE Sel. Areas Commun.*, 1998, **16**, pp. 1309–1319
- 6 SOTOBAYASHI, H., CHUJO, W., and KITAYAMA, K.: 'Demonstration of ultra-wideband and transparent virtual optical code/wavelength path network'. OFC 2001, 2001, Paper TuV
- 7 KITAYAMA, K., WADA, N., and SOTOBAYASHI, H.: 'Architectural considerations for photonic IP router based upon optical code correlation', *IEEE/OSA J. Lightwave Technol.*, 2000, **18**, (12), pp. 1834–1844
- 8 SOTOBAYASHI, H., and KITAYAMA, K.: 'Transfer response measurements of a programmable bipolar optical transversal filter by using the ASE noise of an EDFA', *IEEE Photonics Technol. Lett.*, 1999, **11**, (7), pp. 871–873
- 9 SOTOBAYASHI, H., and KITAYAMA, K.: '325 nm bandwidth supercontinuum generation at 10 Gbit/s using dispersion-flattened and non-decreasing normal dispersion fibre with pulse compression technique', *Electron. Lett.*, 1998, **34**, (13), pp. 1336–1337
- 10 ASO, O., ARAI, S., YAGI, T., TADAKUMA, M., SUZUKI, Y., and NAMIKI, S.: 'Broadband wavelength conversion using a short high-nonlinearity non-polarization-maintaining fiber'. ECOC'99, 1999, Paper Th B1-5, pp. II-226–227

Integrated optic dispersion slope equaliser for $N \times 20$ Gbit/s WDM transmission

K. Takiguchi, K. Okamoto and T. Goh

The fabrication of a dispersion slope equaliser on a silica-based planar lightwave circuit for 16 \times 20 Gbit/s wavelength division multiplexing transmission is reported. This device comprises an array of sixteen equalisers with different compensation values and an arrayed-waveguide grating for wavelength multiplexing.

Introduction: The growth of the Internet has led to the need for much larger capacity networks. Wavelength division multiplexing (WDM) optical communication systems are the most promising way to achieve this but it is essential to increase their bit rate per wavelength as well as their channel number [1]. Therefore, techniques to compensate precisely for the fibre dispersion slope are becoming increasingly important for such advanced high bit rate WDM systems. Several approaches towards dispersion slope equalisation have been actively investigated with a view to upgrading the capacity of installed fibre cables. These approaches include the use of dispersion-compensating fibres (DCFs), chirped fibre Bragg gratings, and higher order mode fibres [2–5]. The planar lightwave circuit (PLC) dispersion equaliser, which we have developed, has certain unique characteristics, including compactness, dispersion variability, and the ability to provide flexible and accurate dispersion compensation. We previously proposed a disper-